PAPER • OPEN ACCESS

A blended wing body airplane with a close-coupled, tilting tail

To cite this article: R E M Nasir *et al* 2016 *IOP Conf. Ser.: Mater. Sci. Eng.* **152** 012021

View the article online for updates and enhancements.

A blended wing body airplane with a close-coupled, tilting tail

R E M Nasir[*]**, N S C Mazlan, Z M Ali, W Wisnoe and W Kuntjoro**

Aviation Technology Research (ATR) Group, Flight Tech. & Test Centre (FTTC),
Faculty of Mech. Engr. Universiti Teknologi Mara, Malaysia

*rizal524@salam.uitm.edu.my

Abstract. This paper highlights a novel approach to stabilizing and controlling pitch and yaw motion via a set of horizontal tail that can act as elevator and rudder. The tail is incorporated into a new design of blended wing body (BWB) aircraft, known as Baseline-V, located just aft of the trailing edge of its inboard wing. The proposed close-coupled tail is equipped with elevators that deflect in unison, and can tilt – an unusual means of tilting where if starboard side is tilted downward at k degree, and then the portside must be tilted upward at k degree too. A wind tunnel experiment is conducted to investigate aerodynamics and static stability of Baseline-V BWB aircraft. The model is being tested at actual flight speed of 15 m/s (54 km/h) with varying angle of attack for five elevator angle cases at zero tilt angle and varying sideslip angle for four tilt angle cases at one fixed elevator angle. The result shows that the aircraft's highest lift-to-drag ratio is 32. It is also found that Baseline-V is statically stable in pitch and yaw but has no clear indication in terms of roll stability.

1. Introduction

Blended wing body (BWB) aircraft configuration can offer reduction in fuel consumption and noise by reducing drag [1]. It has a lifting body, instead of tubular fuselage, blended smoothly to its wing, thus increases lift force. The smooth transition between body and wing reduces interference drag and its low wetted surface area compared to conventional aircraft of the same volume reduces skin-friction drag. The combination of high lift and low drag forces increases the lift-to-drag ratio (L/D) of BWB aircraft up to 20% more than conventional aircraft [2, 3]. However, high L/D of BWB aircraft design can only be practical with careful attentions to other important requirements such as flight stability and control. Despite aerodynamic advantages, BWB aircraft can become statically unstable due to short moment arm between control surface to its centre of gravity [4]. BWB aircraft have similar stability and control issues as flying-wing designs [5] and these are made worse by its sensitivity to external disturbances such as gust [6]. It is usually designed with multiple elevons located almost at full wing span because it needs large control surface area to counter its nose-down pitch moment generated by its lifting body and wing combined [7]. Just like what has been discussed in [3], a pure tail-less BWB aircraft is not only very challenging to be designed if one were to have good balance between L/D and stability, the intricate "blending" of lifting body and tail makes fabrication of aircraft structures or its wind tunnel model complex and expensive [8].

Bolsunovsky *et al.* [3] propose various plan forms and tail configurations for BWB aircraft due to inadequate control in yaw. This makes the BWB aircraft looks conventional, not to mention additional drag created by the twin vertical tails that increase interference drag. A new solution has to be found regarding inadequate yaw stability and controllability and one may look at nature to be inspired. A bird

does not have vertical tail like conventional aircraft but it is still be able to control its yawing motion by tilting its tail with combination of tail pitch angle [9].

2. Design concept

A novel approach is proposed in this study to stabilize and control pitch and yaw motion via a set of horizontal tail that can act as elevator and rudder. The said tail is incorporated into a new design of BWB aircraft, known as Baseline-V, located just aft of the trailing edge of its inboard wing as shown in Figure 1. The proposed close-coupled tail is equipped with elevators that deflect in unison (port and starboard side deflect at the same angle η at the same direction), and can tilt – an unusual means of tilting where if starboard side is tilted downward at k degree, then the portside must be tilted upward at k degree too. Figure 2 shows how the elevator is deflected and the tail is tilted. Deflection of elevator angle alone can only stabilize (or trim) and control the said aircraft in pitch. Tilting the tail rotates the direction of tail lift (or down force) to an angle normal to tail plane. This produces a component of force sideways thus producing yawing moment that causes the aircraft to yaw and also roll (due to small rolling moment produced). Figure 3 shows how the combination of elevator angle deflection and tail tilt can theoretically causes this phenomenon. Increase in tilt angle shall theoretically increase yaw moment that yaw control shall be possible without using any rudder hence there shall be no need for a vertical tail.
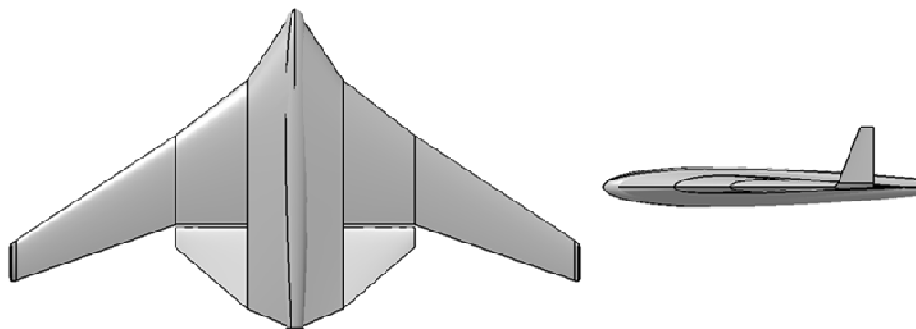

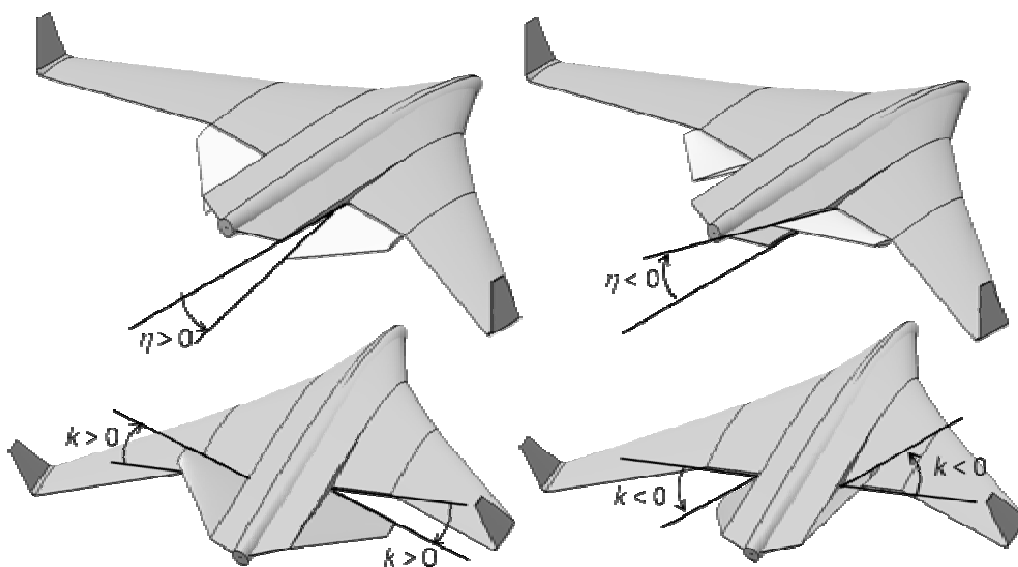**Figure 1.** Baseline-V BWB with a close-coupled tail – plan and side views

Figure 2. Drawings show elevators at angle η and tails tilt at angle k
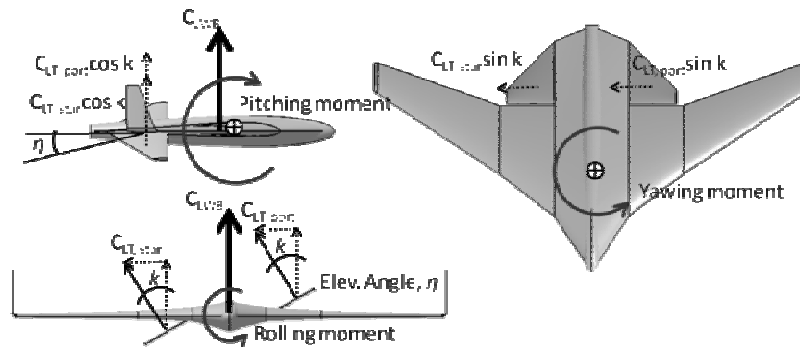
Figure 3. Schematics of theoretical effect of elevator deflection and tail tilt

The main reason for coming up with the design is to have yawing control without having a rudder on vertical tail. It is found that incorporating rudder on winglet is impractical as it requires tiny but powerful servo, which can be very expensive. Inspired by tilting tail of a bird, this solution is found where the tail can be used as pure elevator if it is horizontal, and can also act as rudder if the tail is tilted. This is impractical for big airline-sized aircraft but it is suitable for a small drone proposed here.

From plan view, the BWB seems like a tail-less aircraft just like other BWBs and hypothetically, small gap between trailing edge of the inboard wing and the nose of the tail may eliminate interference drag, thus maintaining its high L/D. How is this possible? Conventional wing-body-tail configuration has its tail located far away from the wing and the top and bottom airflow past the wing is reunited. After reuniting for quite some length, the airflow passes the horizontal tail hence; in this case, the tail becomes another "obstacle" to the airflow. On another aspect, the horizontal tail sticking out clearly from the body disrupts smooth airflow around the body and interference drag is expected. In addition, conventional tails (horizontal and vertical) add frontal area of the whole aircraft. For Baseline-V, the tail is so close that, theoretically, the top and bottom airflow on inboard wing may not be reunited and continues to flow on top and bottom of the tail separately as if the tail is integral part of the wing. It is like having a slotted flap behind the wing but in this case, it is not connected physically to the wing because it needs to be tilted to act as rudder. However, most of Baseline-V cruising time will have its tail staying horizontal at k = 0 degree with some elevator angle η for angle of attack trim. High aerodynamic efficiency (read: lift-to-drag ratio) is expected here because the wind (airflow) does not "see" the tail. However, drag is expected to increase when the tail begins to tilt because aircraft frontal area is increased thus lift-to-drag ratio is expected be reduced significantly.

3. Experiment setup
The objective of this experiment is to investigate aerodynamics and static stability of Baseline-V BWB aircraft. To achieve this, data of forces and moments in all six axes, namely longitudinal, side and vertical forces and roll, pitch and yaw moments, are collected at each angle of attack α and/or angle of sideslip β, for each elevator angle η and tilt angle k with airspeed similar to the aircraft's designed cruising/loitering speed. The experiment is conducted in a low speed wind tunnel (UTM-LST) at the Aeronautic Laboratory of Universiti Teknologi Malaysia (UTM). Raw data of forces and moments collected is then converted into coefficients that will be corrected for buoyancy, solid blockage and wake blockage. Drag, side force and lift coefficients represent the aerodynamic force to analyze their curve trends, slopes, extrema, intersections and most importantly to be converted into measurement of aerodynamic efficiency in terms of lift-to-drag ratio, L/D while pitch and yaw moment coefficients represent aerodynamic moments used to analyze static stability.

Baseline-V BWB is a small UAV for surveillance mission. The wind tunnel model is fabricated from pine woods, some lightweight plywoods, carbon fibre rods, balsa skin and plastic coverings, and is build to 1:1 scale. In fact, the wind tunnel model is build in similar manner to the actual UAV itself. Table 1 highlights the geometric specifications of Baseline-V.

Table 1. Wing-body and tail design parameters

Wing-body		Tail	
25% sweep	30^0	25% sweep	-12.05^0
Wing area, S	0.4 m^2	Tail area, S_t	0.05 m^2
Wing span, b	1.4 m	Tail span, b_t	0.36 m
Aspect ratio, AR	4.92	Aspect ratio, AR_t	2.60
Mean chord, c	0.284 m	Mean chord, c_t	0.127 m

The wing-body design can generally be divided into three main segments: body, inboard wing and outboard wing. The body is designed based on standard symmetrical airfoil section modified at the trailing edge to provide nose up pitch moment. Similarly, for inboard and outboard wing sections, the modification is also made to their respective airfoil sections near trailing edge to reduce the negative pitch moment coefficient normally found on standard 12-percent and 15-percent thickness-to-chord cambered airfoils. Again, this is done to reduce nose down moment that is prevalent on swept-back wing. The aspect ratio of this aircraft (body included since it also generates lift) is generally medium at 4.92, which is similar to some general aviation airplanes. The inboard-outboard wing combo has a planform similar to common airliners of today. The trailing edge of the inboard wing is less than five millimetres from leading edge of the tail. The tail is originally designed from standard symmetrical airfoil sections but it is then changed to a mere plate with rounded leading edge for practicality reason. The Baseline-V BWB is also equipped with vertical wing tips, mainly for reducing the trailing edge vortices' size, hence improving lift-to-drag ratio but also contribute to ensuring yaw stability especially when the tail is not tilted (horizontal). Without the wing tip, directional static stability depends on the planform shape of the BWB alone and since without it, the aircraft has small side area and couple with short length of its body relative to its wing span, the aircraft may have large tendency to spin out of control or "boomerang".

The closed circuit wind tunnel used in this study has a test section of 1.5 m x 2 m x 5.8 m. This tunnel can operate at wind speed between 3 m/s to 80 m/s. Full scale wind tunnel model of Baseline-V with control surfaces that can be deflected remotely is mounted on three struts connected to turntable on the floor as shown in Figure 4. The turntable is mounted on balance with sensors to measure forces and moments of aircraft at varying angle of attack α and sideslip angle β. The aft pitching strut was connected to the model using a single boom. Since the model tested is an actual size of the UAV, the results obtained in this experiment are assumed to be the actual aerodynamic behaviour of Baseline-V BWB. The model is being tested at actual loitering flight speed of 15 m/s (54 km/h) and Reynold's number, Re = 263,000 at its mean chord, which indicates a laminar flow. The range of Reynold's number from wing tip to the body centre section is between 120,000 to 600,000. While most of the spanwise wing-body sections are in laminar flow, there are sections especially on the body that is within transition between laminar and turbulent flow. In the meantime, the Mach number of the test is around 0.05, thus compressibility effect can be ignored. The experiment is divided into two major segments:

- varying angle of attack for five elevator angle cases at zero tilt angle ($-10° \leq \alpha \leq +10°$; $\eta = -20°, -10°, 0°, +10°, +20°$; $k = 0°$)
- varying sideslip angle for four tilt angle cases at one fixed elevator angle ($-10° \leq \beta \leq +10°$; $k = 0°, +15°, +30°, +45°$; $\eta = 0°$).

The first segment is aimed at looking for the effect of elevator angle cases to lift and drag coefficients, aerodynamic efficiency and pitch moment static stability in a simulated straight (zero sideslip angle), steady and level flight condition while the second is for the effect of tail tilt angle at fixed angle of attack but varying sideslip angle to side force, drag and yaw moment in a simulated crosswind flight condition.
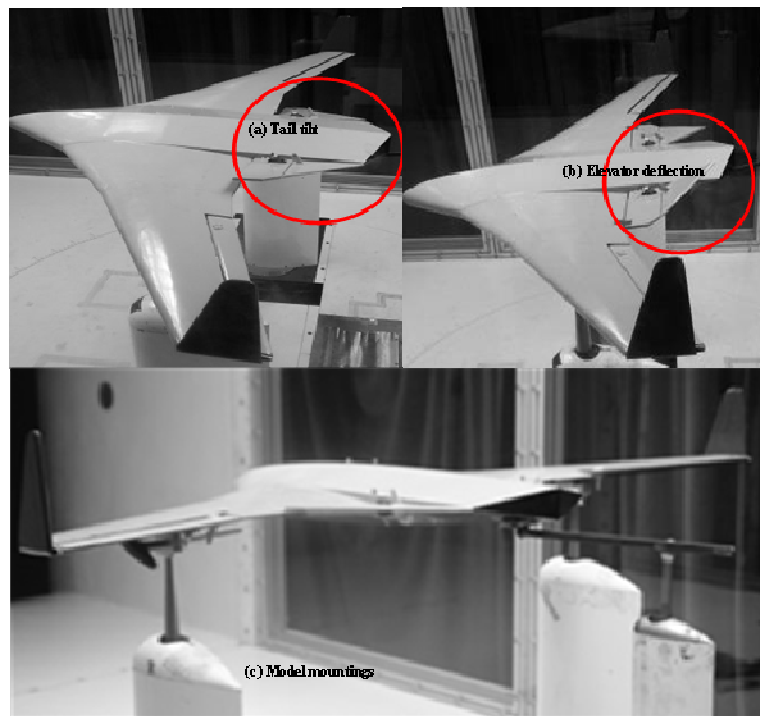
Figure 4. Baseline-V BWB (a) tilting the tail (b) elevator deflection (c) mountings

4. Results

Figure 5 shows four plots that represent the effects of elevator angle to the BWB aircraft at zero tilt angles. These are plotted to examine the effect of elevator angle to lift versus angle of attack trend (C_L vs α), drag polar trend (C_L vs C_D) and aerodynamic efficiency (L/D vs α), and also to determine pitch stability and suitable trim lift (trim angle of attack) at steady and level cruise condition.

C_L versus α plots shows almost all elevator cases have near linear trend except for $\eta = 0°$ for angles of attack within $-10° \leq \alpha \leq +10°$. There is significant increase of C_L as η increases i.e. increment of $\Delta C_L \sim 0.3$ from $\eta = -20°$ to $\eta = +20°$ roughly averaging the change of C_L with respect to the change of η to $dC_L/d\eta \cong 0.0075$ per degree. The average slope of C_L versus α plot for all cases is around 0.08 per degree or 4.58 per radian. This is 27% less than the theoretical ideal lift curve slope of 2π per radian and this can be considered steep for a BWB airplane that has aspect ratio less than 5.0. From experiences in previous studies, the lift curve slope for low-aspect ratio to medium-aspect ratio BWB airplane usually ranges from 0.04 to 0.06 per degree. Meanwhile, angles of attack at zero lift $\alpha_{CL=0}$ ranges from near $-5°$ to $-2°$, which is a normal range for a wing.

As for drag polar plot, it is expected that the lowest drag shall belong to $\eta = 0°$ case with its lowest drag coefficient C_D is lower than 0.02 and happens at $C_L \sim 0.5$, which corresponds to $\alpha = +3°$. For other η cases, the lowest C_D also occurs at near $\alpha = +3°$ but with higher magnitude of C_D than $\eta = 0°$ case. Increase in absolute elevator angle ($|\eta|$) also increases C_D, thus agreeing with the conventional understanding that larger elevator angle creates larger drag at all angles of attack. The minimum C_D for each drag polar cases does not happen at zero C_L but rather at around $C_L \sim 0.5 - 0.8$ indicating that the BWB aircraft in study is of "cambered-type". Optimal C_D (the lowest drag at a given lift, C_{Dopt}) seems to be at a point where $C_L \sim 0.5$ but one must look at L/D versus α plot to be sure.

From L/D versus α plot, the highest L/D happens at angle of attack near $\alpha = +3°$ with the highest recorded L/D ~ 32 for $\eta = 0°$ case. This means that for optimal flight C_L of 0.5 the C_D is 0.015. The drag coefficient at maximum L/D is actually rather normal for a clean, sleek airplane but the high L/D is attributed to the Baseline-V high lifting capability. The other elevator angle cases see large drop of
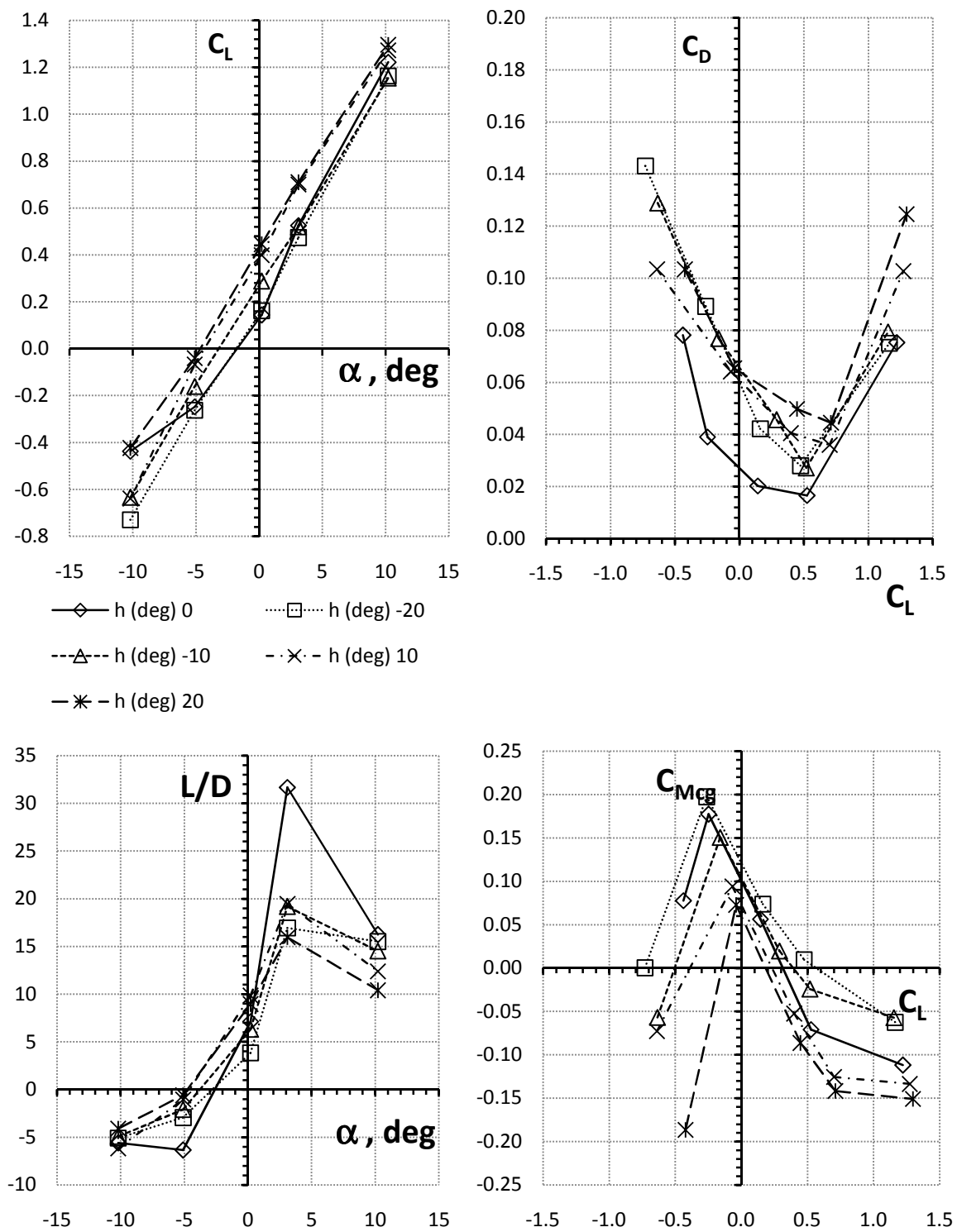
Figure 5. C_L versus α, C_D versus C_L, L/D versus α and C_{Mcg} versus C_L plots

maximum L/D to just 15-20 and even this is higher than many aircraft's L/D. As expected, the most suitable trim angle of attack α_{trim} to fly is at around $\alpha = +3°$ that give the highest L/D – i.e., if the mass of this Baseline-V BWB UAV is around 3.2 kg, then the propulsive thrust needed to overcome the drag at this trim angle is just 100 grams! However, a slight increase or decrease in angle of attack causes large drag increment, subsequently a quick drop of L/D ratio. In real flight of a remote control airplane of this design with such a small wing span, trimming at angle of attack that gives the highest L/D is one major problem. The designed UAV is susceptible to wind gust and change in airspeed – both of which change its angle of attack – hence reducing its lift or increasing its drag fairly quickly.

In the context of flow regime, it is mentioned that the Reynold's number at the mean chord is Re = 263,000 while range of Reynold's number from wing tip to centre body is Re = 120,000 to 600,000. This corresponds to the average laminar skin friction coefficient $C_f = 0.0026$ at mean chord, which is around 17% of the total drag coefficient at $\alpha = +3°$ that is 0.015. Laminar skin friction from centre body section to wing tip is $C_f = 0.0017$ to $C_f = 0.0038$ or 11.3% to 25.3% of just mentioned drag coefficient. Such a low average skin friction coefficient is one of the reasons for high L/D of 32.

However, pitch moment versus lift coefficients (C_{Mcg} versus C_L plots) show that at current centre of gravity (C.G.) location (or centre of turntable for wind tunnel experiment), the trim C_L (or C_L at $C_{Mcg} = 0$) for all η cases does not fall at its optimal $C_L \sim 0.5 - 0.8$ that give the highest *L/D* but rather at lower range of C_L. For instance, elevator angle of $\eta = 0°$ case has trim lift at $C_L \sim 0.3$, which is at around $\alpha \sim +2°$ with $L/D \sim 25$ only. Generally, all η cases have negative slope ($dC_{Mcg}/dC_L < 0$) with positive C_{Mcg} at $C_L = 0$ ($C_{M0} > 0$) for $-5° \leq \alpha \leq +10°$ indicating that the Baseline-V is longitudinally, statically stable. Rough average dC_{Mcg}/dC_L slope is around 0.25 – 0.30 meaning that static margin, where the aerodynamic centre of the whole aircraft (or neutral point) is approximately 25% - 30% of mean chord behind the C.G. This can further be 'relaxed' by shifting the C.G. back around 10% of mean chord to trim the aircraft at $\alpha = +3°$ where its lift-to-drag ratio is the highest.

The second part of this experiment embarks on observing the effect of tilt angle k to the drag coefficient C_D, side force coefficient C_Y, yaw moment coefficient C_{Ncg} and roll moment coefficient C_{Lcg}. These coefficients are measured with variation of sideslip angle β to observe trends and slopes $dC_D/d\beta$, $dC_Y/d\beta$, $dC_{Ncg}/d\beta$ and $dC_{Lcg}/d\beta$ that determine the hypothesis regarding increased of drag with increased in tilt angle mentioned earlier, how side force changes with sideslip angle, yaw stability and roll stability, respectively.

Figure 6 shows two plots - C_D versus k (left) and C_Y versus β (right). The drag coefficient C_D versus tilt angle k plot highlighted here is for zero elevator angle $\eta = 0°$ cases at fixed angle of attack $\alpha \sim 2°$ and zero sideslip angle $\beta = 0°$. This is to prove that the drag increases with tail tilt angle k, which increases exposed tail frontal area. At $k = 0°$ or when the tail is completely horizontal and hides behind the inboard wing, the $C_D \sim 0.011$ only. At $k = \pm 15°$ when some of the tail is exposed from frontal view the drag coefficient increases by 0.004 or 36.3%. Increasing absolute tail tilt angle by another 15 degrees to $k = \pm 30°$ sees a sudden jump in drag coefficient to 0.027 or 245% of the drag coefficient when the tail is completely horizontal, indicating at this tilt angle there is a larger frontal tail area exposed creating larger obstacle to top and bottom layers of the free airflow farther from the inboard wing surfaces. This is a sign of interference drag existence, therefore, is a proof of earlier hypothesis claiming that close-coupled horizontal tail can reduce interference drag. Increasing tail tilt angle to $k = \pm 45°$ increases drag coefficient by a slight 0.001. This can be considered insignificant because at $k = \pm 30°$, much of the frontal area of the tail has been exposed already and increased in further $\pm 15°$ in k does not changed the exposed area by much.

The right plot of Figure 6 shows the side force coefficient C_Y versus sideslip angle β for various cases of tail tilt angle k. Positive side force means that the force is directed to the starboard side or right side with positive sideslip angle is when the wind comes from the starboard or right side. General trend of these C_Y versus β curves is nearly linear with negative slopes averaging around -0.006 per degree of β. Increasing sideslip angle decreases sideslip force value, but this does not mean there is no side force at high sideslip angle. Since both sideslip angle and side force are actually vector quantities

this would mean as absolute sideslip angle in one direction is increased then the sideslip force is also increased in the opposite direction. In Baseline-V case the side force coefficient is quite large at 0.08 even at only $= \pm 10°$. This is larger than drag coefficient of 0.07 at $\alpha = \pm 10°$ for $\eta = 0°$ case. This means that a sizable rudder is needed to counter side drifting of this aircraft during crosswind.

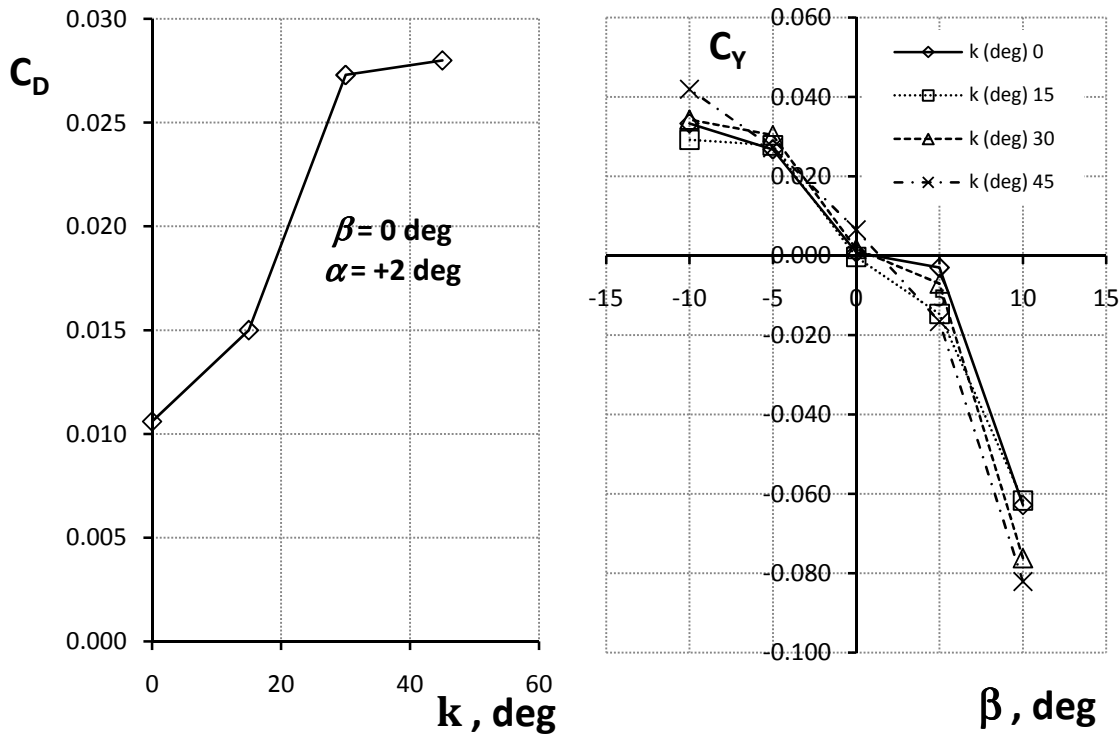**Figure 6.** C_D versus k (left) and C_Y versus β (right)

Increasing tail tilt angle k is surely causing exposed side area of the aircraft to increase thus increasing the absolute value of side force. As the tail tilt angle is increased, the increase in side force (absolute value of C_Y) is 0.00033 per degree of k at $\beta = \pm 5°$ and 0.00044 per degree of k at $\beta = \pm 10°$. However, the change in side force coefficient due to changing tail tilt angle is not much larger than the effect of the aircraft's planform-vertical wing tip combo in generating side force with respect to sideslip angle at -0.006 per degree of β mentioned earlier which is more than ten times the effect of tail tilt angle to the side force. This is because the side form wing-body area and vertical wing tip area is larger than side view area of tilting tail thus they play major role in generating side force and are influential in determining how side force is enlarged with increasing sideslip angle.

Figure 7 shows two important plots related to the effect of k to C_{Ncg} and C_{Lcg} at fixed $\eta = 0°$ and fixed $\alpha = +2°$ that represent near optimal cruise condition with $L/D \sim 25$ as mentioned before. C_{Ncg} versus β plots shows that, for all k cases, the slope $\mathrm{d}C_{Ncg}/\mathrm{d}\beta$ is positive. Therefore, the aircraft is directionally, statically stable. There seems to be small but significant differences in C_{Ncg} magnitude between k cases – C_{Ncg} is larger for larger k and this seems to agree with theoretical hypothesis shown in Figure 3. Logically, as k is increased, larger tail side force is generated while lower tail lift is to be expected. The trend of C_{Ncg} versus β plots also agrees with conventional understanding that as β is increased, C_{Ncg} also increases. However, the magnitude of C_{Ncg} is small relative to C_{Mcg}.
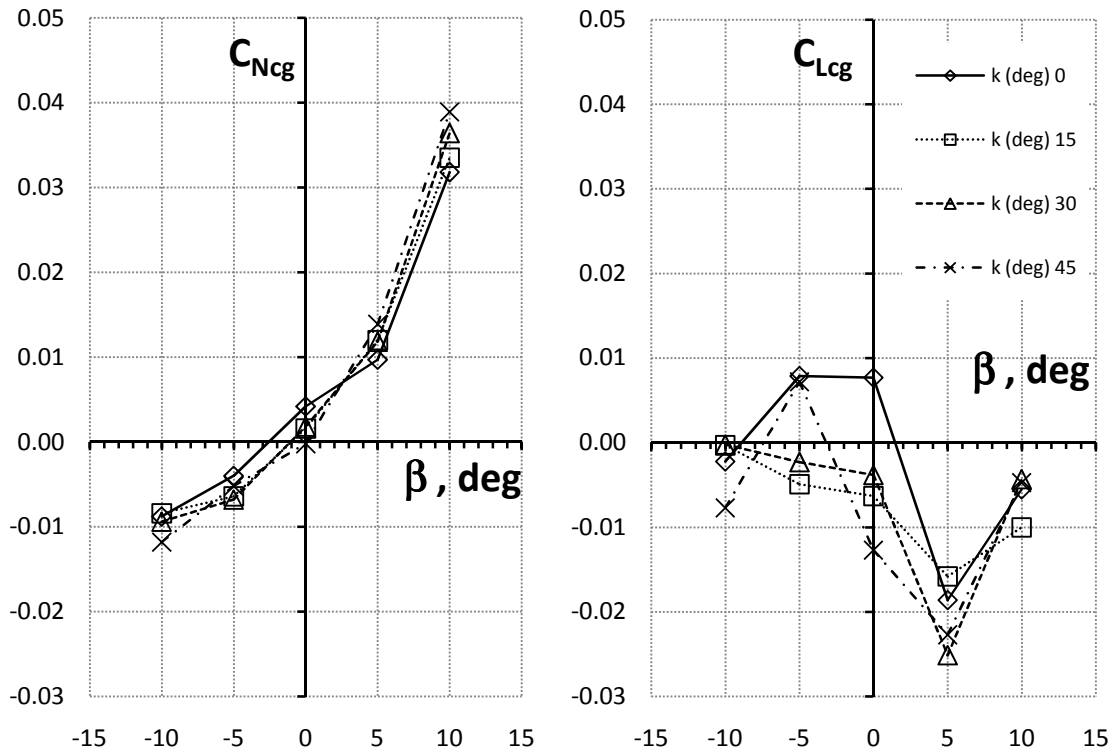
Figure 7. C_D versus k (left) and C_Y versus β (right)

Plot of rolling moment versus sideslip angle (C_{Lcg} versus β) on the right side of Figure 7 shows unclear trend. It is expected to be near linear with $dC_{Lcg}/d\beta < 0$ but it is not so in Baseline-V BWB case, although negative C_{Lcg} is observed at positive value of β while positive C_{Lcg} is found in most cases for negative β. The negative $dC_{Lcg}/d\beta$ within low β magnitude region shows some capability to return to level wing condition. However, knowing that Baseline-V has mid-wing and mid-tail setup, it is fair to say that the rolling moment slope shall be flat or $dC_{Lcg}/d\beta = 0$ (neutrally stable) and tilting the tail in this case may not change its rolling stability.

5. Concluding remarks

The change of lift coefficient with respect to the change of elevator angle η is approximately +0.0075 per degree. The average lift curve slope for all cases is around 0.08 per degree or 4.58 per radian of angle of attack. Angles of attack at zero lift $\alpha_{CL=0}$ ranges from near $-5°$ to $-2°$. The lowest drag coefficient is lower than 0.02 (at round 0.015) and happens at lift coefficient of approximately 0.5, which corresponds to $\alpha = +3°$. In other η cases, the lowest drag coefficient also occurs near $\alpha = +3°$ but with higher magnitude than $\eta = 0°$ case. With this BWB design, the highest L/D is recorded at 32, which is very high for such an aircraft with moderate aspect ratio. One of the reasons for high lift-to-drag ratio is its low friction coefficient, which is only around 17% of total drag coefficient due to the aircraft flying within laminar flow regime. It is proven that having close-coupled horizontal tail right behind the inboard wing reduces interference drag. As the tail is tilted the exposed frontal area of tail creates a new obstacle that increases drag. Trend of side force coefficient versus sideslip angle curves is nearly linear with negative slopes averaging around -0.006 per degree of β. As the tail tilt angle is increased, the increase in side force is 0.00033 per degree of k at $\beta = \pm 5°$ and 0.00044 per degree of k at $\beta = \pm 10°$. There seems to be small but significant differences in the yawing moment coefficient magnitude between k cases, where yawing moment is larger for larger k and this seems to agree with theory shown. Finally, there is no clear trend regarding rolling moment versus sideslip angle.

From general observation here, it is appropriate to mention that Baseline-V, a BWB aircraft with close-coupled tilting tail, is statically stable in pitch and yaw but has no clear indication in terms of rolling stability. In addition, the elevator at $\eta = 0°$ has the largest L/D. It is recommended to shift the C.G. slightly closer to aircraft neutral point such that its dC_{Mcg}/dC_L slope shall be less steep and trim at exactly $\alpha = +3°$ to fly at L/D $\sim$ 32 where Baseline-V BWB can cruise at the lowest required thrust and saves energy, thus increases range and endurance.

Acknowledgment

References

[1]   Liebeck R H 2004 *J. Aircraft* **41** 10-25
[2]   Qin N, Vavalle A, Le Moigne, Laban M, Hackett K and Weinerfelt P 2004 *Prog. Aerosp. Sci.* **40** 321–43
[3]   Bolsunovsky N, Buzoverya B, Gurevich V, Denisov A, Dunaevsky L, Shkadov O, Sonin U and Zhurihin J 2001 *Aircr. Design* **4** 193–219
[4]   Nasir R E M, Kuntjoro W and Wisnoe W 2014 *Procedia Tech.* **15** 784–792
[5]   Karakas H, Koyuncu E and Inalhan G 2013 *Journal of Intelligent and Robotic Systems* **69** 131-46
[6]   Cai C F, Wu J H and Liang B 2014 *Adv. Mater. Res.* **1016** 359–64
[7]   Li P, Zhang B, Chen Y, Yuan C and Lin Y 2012 *Chinese J. Aeronaut.* **25** 508–16
[8]   Mat S, Ishak I S, Zakaria K and Khan Z A 2014 *Adv. Mater. Res.* **845** 971–4
[9]   G. Sachs G 2005 *J. Theor. Bio.* **234** 471–8